

Detection and attribution of extreme precipitation changes from 1961 to 2012 in the Yangtze River Delta in China

Fengsong Pei^a, Changjiang Wu^a, Xiaoping Liu^{b,a,*}, Zhaoling Hu^a, Yan Xia^a, Li-An Liu^a, Kun Wang^a, Yi Zhou^a, Li Xu^a

^a School of Geography, Geomatics and Planning, Jiangsu Normal University, Xuzhou 221116, PR China

^b Guangdong Key Laboratory for Urbanization and Geo-simulation, School of Geography and Planning, Sun Yat-sen University, Guangzhou 510275, PR China

ARTICLE INFO

Keywords:

Extreme precipitation events
Peaks-over-threshold
Generalized Pareto distribution
Trend attribution
Yangtze River Delta

ABSTRACT

Extreme climatic changes frequently have more serious impacts on nature and human society than do changes in the mean value under global climate change. However, extreme climatic events, particularly extreme precipitation, show complex variability because of the effects of natural and human impacts. Taking the Yangtze River Delta (YRD) in China as a case study, the characteristics and trends of extreme daily precipitation events from 1961 to 2012 were investigated in terms of their frequency and intensity. The extreme precipitation events at 30-year and 50-year return periods were analyzed by assuming a generalized Pareto distribution. The detection and attribution of extreme precipitation changes were conducted via the simultaneous evaluation of gradual and abrupt changes.

The results indicate a similar pattern of extreme daily precipitation events during different return periods, but the differences in the daily precipitation extremes are quite larger between stations. Thus, regional analyses of different return periods are needed to minimize the risks and losses from extreme precipitation events. We also found reversed trends of extreme daily precipitation events in the YRD when assuming gradual and abrupt changes over the period of 1961–2012. The trend attribution analyses showed that a large-scale monsoon might play a critical role in the intensity and frequency of extreme daily precipitation events in the YRD. However, local factors (e.g., typhoons and urbanization) might play an important role in extreme precipitation changes under a monsoon background.

1. Introduction

Past studies have shown that the global air temperature has risen by approximately 0.74 ± 0.18 °C during the last 100 years (Solomon et al., 2007). This warming is projected to continue, and is likely to be accompanied by climatic events (e.g., severe flooding, drought, and heatwaves) (Houghton et al., 2001; Cai et al., 2014). Extreme climatic events often exert serious impacts on society, economy and ecosystems than do changes in the mean value because of agricultural damage and even loss of life (Heisler White et al., 2009; Taylor et al., 2013; Tomczyk et al., 2015; Pei et al., 2018). An extreme climatic event refers to the occurrence of a climatic variable above (or below) a given threshold near the upper (or lower) ends of a sequence of observed values of the variable (IPCC, 2012). It is difficult to better understand the behavior of extreme climatic events (e.g., extreme precipitation) (Sarhadi and Soulis, 2017).

During recent decades, extreme precipitation events have received

increasing attention among the scientific community throughout the world. For examples, Herold et al. (2016) assessed daily precipitation extremes in the tropics and subtropics by using precipitation indices. Sunyer et al. (2015) analyzed changes in extreme precipitation events in Europe using statistical downscaling methods. Tedeschi et al. (2016) investigated seasonal, monthly mean precipitation and extreme events in South America. Wu et al. (2016) evaluated the trends in summer extreme precipitation over East Asia using four regional climatic models. The characteristics and trends of extreme precipitation events are complex and vary between regions at different scales throughout the world.

The Yangtze River Delta (YRD) is the most developed and densely populated region in China. It frequently experiences daily precipitation extremes and floods. However, the variability in extreme precipitation events, as well as its causes in the YRD remain uncertain according to observed records and model simulations. For example, Zhang et al. (2008) assessed changes in extreme precipitation events in the YRD by

* Corresponding author at: School of Geography and Planning, Sun Yat-sen University, 135 West Xingang RD., Guangzhou 510275, PR China.
E-mail address: liuxp3@mail.sysu.edu.cn (X. Liu).

comparing ECHAM5/MPI-OM model results and observed data. They argued that there were no significant trends in extreme precipitation from 1951 to 2000. Yin et al. (2016) analyzed the spatial patterns of extreme precipitation events with a 100 year return period in the YRD. They found that most observations of precipitation extremes in the region have no significant trends. Han et al. (2015) analyzed trends in annual and seasonal precipitation extremes in the YRD during the period of 1957–2013. Hu et al. (2016) evaluated the long-term trends of daily precipitation in the YRD from 1960 to 2012 by using 12 precipitation indices. They found that nine indices showed increasing trends, while three indices showed decreasing trends. Past studies have frequently examined the trends in extreme precipitation events by assuming a monotonic change. However, climatic variables may not conform to this assumption (Yang and Tian, 2009; Zhang et al., 2009; Ehsanzadeh et al., 2015). Different studies have even reached conflicting conclusions when operating with changes in extreme precipitation events during past decades in the YRD.

In this study, return period analysis was employed to estimate the likelihood of extreme event occurrence, and identify the potential risk of extreme daily precipitation events in future decades. We aimed to examine the characteristics, gradual and abrupt changes of extreme daily precipitation events in the YRD from 1961 to 2012, and attribute them to aspects of the East Asian summer monsoon (EASM), tropical cyclones (i.e., typhoons), large-scale urban land use, and a local topographic factor.

2. Study area and data preprocessing

2.1. Study area

The study area is located in the Yangtze River Delta (YRD) (Fig. 1). It lies between 118°E–123°E and 28°N–34°N and has an area of 104,985 km². The YRD encompasses the entire city of Shanghai, the southern parts of Jiangsu Province, and the northern parts of Zhejiang

Province. The average elevation is less than 10 m in the northern YRD region. Some mountains occur in the southern YRD and have a maximum elevation of 1500 m (Fig. 1). The YRD region is a typical monsoonal climatic region and is influenced by the East Asian monsoon. The annual total precipitation ranges from 1024 mm at Gaoyou station to 1925 mm at Kuocangshan station. In terms of socioeconomic aspects, the population reached 110.8 million in 2016. In addition, the gross domestic product (GDP) reached US\$1.74 trillion, accounting for 16.2% of the total GDP in China. Thus, the YRD is among the important vulnerable zones in terms of the exposure of such large population and economic assets to extreme precipitation events in China.

2.2. Data and preprocessing

Daily precipitation data from 1961 to 2012 were obtained by stations from the Chinese Meteorological Data Service Center (CMDC), China Meteorological Administration (CMA). The quality control of the data was first conducted by the CMDC via manual inspection of time consistency and extremum validation (CMA, 1979). We further validated the data by screening and eliminating suspicious and missing records to ensure their continuity and consistency. For relocated stations such as Baoshan and Longhua stations in Shanghai, we combined the records of daily precipitation measurement from both stations. Consequently, a total of 16 stations, nearly evenly-distributed in the YRD, were selected for further analysis (Fig. 1).

In addition, data on the East Asian summer monsoon, typhoons and urban land use were also collected. We obtained the East Asian summer monsoon index (EASMI) data from the College of Global Change and Earth System Science (GCESS) (GCESS, 2017). The best track records of tropical cyclones, including their positions as well as movement and intensity (e.g., typhoons) in the western North Pacific, were obtained for the period of 1961–2012 from the Regional Specialized Meteorological Center (RSMC) Tokyo-Typhoon Center (RSMC, 2017). Night-time DMSP/OLS satellite images of city lights in 2006 were obtained

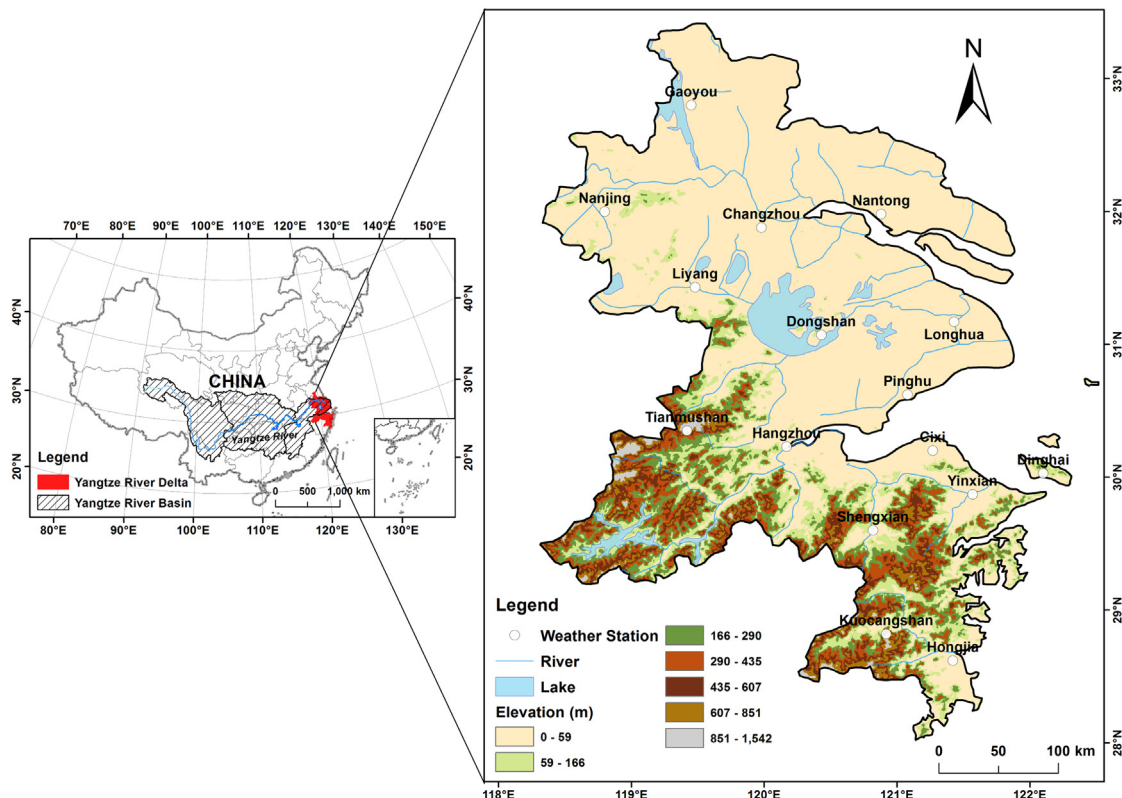


Fig. 1. Location of the Yangtze River Delta.

Table 1
Dataset used in this study.

Dataset	Resolution	Time-interval	Sources
Precipitation	Daily, site-based	1961–2012	CMDC, CMA
EASMI	Monthly & yearly	1961–2012	GCESS
Tropical cyclones records		1961–2012	Tokyo-Typhoon Center
DMSP/OLS images	Yearly, 30 arc-second	1961–2012	NCEI, NOAA

from the National Centers for Environmental Information (NCEI) website in the U.S. (NCEI, 2017). The datasets used in this study are listed in Table 1.

3. Methods

3.1. Peaks-over-threshold approach to identify extreme daily precipitation events

The peaks-over-threshold (POT) approach, which considers the exceedance of all sample values over a given threshold, was employed to identify extreme daily precipitation events. The resulting data series was further fitted to exponential or generalized Pareto distributions (GPD) (Coles et al., 2001; Cunnane, 1973). The GPD, introduced by Pickands (1975), has been widely used in studies dealing with extreme precipitation events (Wang, 1991; Acero et al., 2011). For a random variable x ($x \geq u$), the cumulative probability function for the GPD is as follows:

$$F(x) = \begin{cases} 1 - \left(1 + \frac{\xi(x-u)}{\sigma}\right)^{-1/\xi}, & \xi \neq 0 \\ 1 - \exp\left(-\frac{x-u}{\sigma}\right), & \xi = 0 \end{cases} \quad (1)$$

where u is the location parameter, and σ and ξ denote scale and shape parameters, respectively.

The location parameter of the GPD, which is unrelated to the mean of the distribution, is frequently equal to a threshold of extreme events during a given period (Valadares Tavares and Evaristo Da Silva, 1983; Donegan et al., 2013). In this study, the threshold is defined as the daily precipitation amount of the 95th percentile of the cumulative frequency distribution (Zhai et al., 2005; Su et al., 2008; Lupikasza, 2016). For the scale parameter, higher scale parameter estimates are frequently associated with higher variability in daily precipitation extremes. Thus, the scale parameter can change with the location parameter in the GPD analysis. The value of the shape parameter (ξ) frequently determines the tail behavior of the GPD. In detail, a positive $\hat{\xi}$ indicates a heavy tail behavior, such as a Pareto distribution. On the other hand, a negative $\hat{\xi}$ shows a light tail behavior, such as a beta distribution. In addition, if $\hat{\xi}$ is equal to zero, it is an exponential type (Kim et al., 2006; Neykov et al., 2014).

The chi-square test has been widely employed to examine the goodness-of-fit of empirical distributions for given data with any probability density function (Lang et al., 1999). In this study, a chi-square test was employed to verify whether the GPD types can adequately represent the observed data of threshold exceedance of extreme daily precipitation events. In detail, the precipitation records from 1961 to 2012 were classified into several classes to compare the distribution of the observed data and GPD. Given significant difference at the level of 95%, five classes were selected according to different quantiles: 0–0.2, 0.2–0.4, 0.4–0.6, 0.6–0.8 and 0.8–1.0.

Considering the auto-correlated behavior of daily precipitation records, dependent events are frequently found by using only naive events above a threshold (Ribatet and Dutang, 2016). Here, if two extreme daily precipitation events spanned less than a 5-day interval, the two events were considered to be dependent, which is also consistent

with other studies (Yang et al., 2008; Schumacher and Davis, 2010). This calculation was achieved using the R software (R Core Team, 2016) including the freely available POT package (Ribatet and Dutang, 2016).

3.2. SEPF and SDPI to analyze extreme daily precipitation events

After identifying the occurrence of extreme daily precipitation events based on the aforementioned threshold, the frequency and intensity of the extreme daily precipitation events were analyzed using a simple index of extreme precipitation frequency (SEPF) and a simple index of extreme daily precipitation intensity (SDPI), respectively (Pei et al., 2017). A simple index of extreme precipitation frequency for a year (SEPF) was calculated as follows:

$$SEPF = \sum_{j=1}^{365} \tau_{yd} \quad (2)$$

$$\tau_{yd} = \begin{cases} 1 & P_d > u \\ 0 & P_d < u \end{cases} \quad (3)$$

where τ_{yd} is a conditional function equal to 1 if the daily precipitation observation P_d on the day d during the year y exceeds the extreme precipitation threshold u . Otherwise, τ_{yd} is equal to zero, indicating the non-occurrence of an extreme daily precipitation event during the period.

To analyze changes in extreme precipitation intensity, a simple index of extreme daily precipitation intensity for one year (SDPI, mm/day) was then calculated as follows:

$$SDPI = \left(\sum_{d=1}^{365} P_{yd} \right) / N_y \quad P_{yd} > u \quad (4)$$

where, P_{yd} (mm) is the precipitation amount on the day d during the year y , u is the threshold to identify the extreme daily precipitation event, and N_y (days) is the number of the extreme daily precipitation events occurring during the year y . Further details regarding the two indices can be found in the studies of Pei et al. (2017).

3.3. Assessment of daily precipitation extremes for different return periods

A probability weighted moments (PWMs) estimator is advantageous to determine the suitable parameters of the GPD function because the PWMs have a lower uncertainty than that of the ordinary moments (Deidda and Puliga, 2009). A distribution function $F = F(X) = P(X \leq x)$ may be characterized by probability weighted moments as follows (Greenwood et al., 1979):

$$M_{i,j,k} = E[X^i F^j (1 - F)^k] \quad (5)$$

Hosking (1990) proposed L-moments, which are more easily related to distribution shape and spread, and are linear combinations of PWMs for any distribution. An approximate estimator of the shape parameter ($\hat{\xi}$) and the scale parameter ($\hat{\alpha}$) for the GPD is determined using L-moments as follows (Hosking, 1990; Palutikof et al., 1999):

$$\hat{\xi} = \frac{l_1}{l_2} - 2 \quad \text{and} \quad \hat{\alpha} = (1 + \hat{\xi})l_1 \quad (6)$$

where l_1 and l_2 are the first two sample L-moments of a random variable X .

A return period denotes the average recurrence interval over an extended period of time based on historical data, and it is usually used for risk analysis (Elquliti et al., 2016). If m denotes the number of samples collected over a number of years and n is the total number of exceedance over the selected threshold u , the mean crossing rate can be estimated as $\lambda = \frac{n}{m}$ without bias. The expression for the number of exceedances during t year is as follows:

$$\lambda_x = \lambda t(1 - F) \quad (7)$$

Taking $(1 - F)$ from Eq. (7), and setting λ_x to unity, and t to T , the quantile x_T , which corresponds to the precipitation during a T -year return period, can be calculated as follows:

$$x_T = \begin{cases} u + \frac{\sigma}{\xi} [1 - (\lambda T)^{-\xi}] & \text{for } \xi \neq 0 \\ u + \sigma \ln(\lambda T) & \text{for } \xi = 0 \end{cases} \quad (8)$$

The algorithm was implemented in R software and the freely available POT package (R Core Team, 2016; Ribatet and Dutang, 2016).

3.4. Detecting the trends in extreme daily precipitation events

In this study, gradual and abrupt changes in extreme daily precipitation events were analyzed at each station, taking the YRD as a whole to examine the temporal-spatial trends. A five-year moving average was calculated to focus on underlying trends rather than short-term shifts. Regarding the gradual changes, monotonic trends of extreme precipitation events were examined over the period of 1961–2012. Regarding the abrupt changes, change-point-analysis was first conducted by using Pettitt's test to detect the mutation year over the period of 1961–2012. The monotonic trends of extreme precipitation events were then examined over the periods before- and after the change point, respectively. After obtaining the monotonic trends of the frequency and intensity of the extreme daily precipitation events, an inverse distance weighted (IDW) interpolation was implemented using ArcGIS (v10.2) to further show the spatial patterns of the trends.

In detail, a Mann–Kendall analysis was employed to examine the monotonic trends of extreme precipitation intensity because of its advantage that samples do not need to follow certain distributions (Hirsch et al., 1982; Zhang et al., 2013). The trend under the Mann–Kendall analysis was evaluated using the standard test statistic Z value as follows:

$$Z = \begin{cases} \frac{S-1}{\sqrt{\text{Var}(S)}} & \text{if } (S > 0) \\ 0 & \text{if } (S = 0) \\ \frac{S+1}{\sqrt{\text{Var}(S)}} & \text{if } (S < 0) \end{cases} \quad (9)$$

where S is the Mann–Kendall test statistic, and $\text{Var}(S)$ is the variance in S . A positive (negative) value of Z indicates an upward (downward) trend. The algorithm was implemented in R software (R Core Team, 2016). The slope of the extreme precipitation intensity was then estimated as the median (Q_{med}) of the N slopes (Q_i) using Sen's slope analysis, as follows:

$$Q_{\text{med}} = \begin{cases} Q_{(N+1)/2} & \text{if } n \text{ is odd} \\ \frac{Q_{N/2} + Q_{(N+2)/2}}{2} & \text{if } n \text{ is even} \end{cases} \quad (10)$$

Further details regarding Mann–Kendall analysis and Sen's slope can be found in the studies of Hipel and McLeod (2005) and Sen (1968), respectively.

Given the discrete nature of the numbers of extreme daily precipitation events, a Poisson regression model was employed to examine the monotonic trends of extreme precipitation frequency in the YRD from 1961 to 2012. In detail, the number of extreme daily precipitation events (N_i) for the year i has a conditional Poisson distribution with the rate of occurrence (λ_i) as follows (Coles et al., 2001; Villarini et al., 2013):

$$P(N_i = k | \lambda_i) = \frac{e^{-\lambda_i} \lambda_i^k}{k!} [k = 0, 1, 2, \dots] \quad (11)$$

To assess the temporal trends in extreme daily precipitation events, the rate of occurrence λ_i was modeled as a linear function of time (by means of a logarithmic link function) as follows:

$$\lambda_i = \exp(a + b \cdot T) \quad (12)$$

where a , b are the regression coefficients. If coefficient b is different from zero at the 5% significance level, statistical evidences can be found to support temporal trends in the occurrence of extreme daily precipitation events.

To detect abrupt changes in extreme daily precipitation events, change-point-detection analyses were conducted in another experiment. In detail, Pettitt's test was conducted to examine a shift in the central tendency of the extreme daily precipitation events (Pettitt, 1979). That is, a statistic $U_{i,T}$ was employed to test whether two extreme precipitation samples (e.g., X_1, X_2, \dots, X_i and X_i, \dots, X_T) originated from the same population as follows.

$$U_{i,T} = \sum_{i=1}^t \sum_{j=i+1}^T \text{sgn}(X_i - X_j) \quad (13)$$

The change point of the series occurs at K_T , which is defined as follows:

$$K_T = \max |U_{i,T}| \quad (14)$$

The details of Pettitt's test can be found in the studies of Pettitt (1979). According to the results of Pettitt's test, the trends during the periods before- and after the change point were further calculated using Mann–Kendall analysis and a Poisson regression model. All of these algorithms were performed using the R software (R Core Team, 2016) and the trend package (Pohlert, 2016).

3.5. Attributing the trends in extreme daily precipitation events

The East Asian summer monsoon (EASM) and tropical cyclones have been found to deeply affect extreme rainfall in China over Asian monsoon areas (Chang et al., 2012; Wang et al., 2016). In this study, the East Asian summer monsoon index (EASMI), developed by Li and Zeng (2002), was employed as an indicator of the East Asian summer monsoon. The EASMI was defined as seasonal- and area-averaged dynamical normalized seasonality (DNS) from June to August at 850 hPa within the East Asian monsoon domain (10°–40°N, 110°–140°E) (Li and Zeng, 2002). This index has been widely employed to measure the East Asian summer monsoon in past studies (Wang et al., 2008; Li et al., 2010). In addition, the effects of tropical cyclones, particularly typhoons, on the occurrence of extreme daily precipitation events were further analyzed during past decades in the YRD. The frequency of typhoons, whose 30 kt winds could cover stations in the YRD (Typhoon Committee, 2008), was then calculated at each stations from 1961 to 2012 using Geographic Information System (GIS). A multi-year average number of typhoons were calculated for the stations in the YRD.

The consequence of urban land use on extreme daily precipitation events was also analyzed by stations. To screen the effects of short-term factors such as anomalous weather, the average intensity and frequency of extreme daily precipitation events were calculated over the period 2000–2012. Corresponding to the extreme daily precipitation events, nighttime DMSP/OLS satellite images of city lights in 2006 were employed to reflect urban land development in the YRD. The average values of the DMSP/OLS satellite images within a 5-km buffer for each station were calculated to represent the level of urban land development around the corresponding stations. Finally, we analyzed the relationships between changes in extreme daily precipitation events, the East Asian summer monsoon, tropical cyclones (i.e. typhoons) and urban land use using statistical analysis at regional-to-local scales.

4. Results

4.1. Chi-square test for examining a generalized Pareto distribution

In this study, a chi-square goodness-of-fit test was used to examine whether the exceedances of the extreme precipitation threshold follow

Table 2
Chi-square test on the generalized Pareto distribution.

Site	Hongjia	Kuocangshan	Shengxian	Yinxian	Dinghai	Cixi
χ^2	1.82	3.13	14.40	1.77	0.85	2.37
P	0.77	0.54	0.01	0.78	0.93	0.67

Site	Hangzhou	Pinghu	Dongshan	Longhua	Liyang	Changzhou
χ^2	3.42	1.39	4.91	0.78	5.55	7.20
P	0.49	0.85	0.30	0.94	0.24	0.13

Site	Nantong	Nanjing	Gaoyou	Tianmushan
χ^2	3.00	1.40	0.38	8.26
P	0.56	0.84	0.98	0.08

a generalized Pareto distribution. According to the chi-square test, we cannot reject the hypothesis that the threshold exceedances of extreme daily precipitation events originate from the generalized Pareto distribution ($P > 0.05$) for all stations except for Shengxian station in Zhejiang Province (Table 2).

4.2. Characteristics of extreme precipitation events in the YRD

Figs. 2, 3 and 4 show the threshold precipitation amount, scale parameter and shape parameter of the GDP concerning extreme daily precipitation events during past decades in the YRD, respectively. As shown in Fig. 2, the threshold of the extreme daily precipitation events is relatively high in the southern and northern parts of the YRD. In contrast, a relatively low threshold appears in the central YRD. In detail, the precipitation threshold reached 42 mm/day at Gaoyou station in Jiangsu Province. It reached 40 mm/day at Nanjing station in Jiangsu Province, and Kuocangshan station in Zhejiang Province. The lowest precipitation threshold was 34 mm/day at Dongshan station in Jiangsu Province and Pinghu station in Zhejiang Province. Despite relatively low annual precipitation at Gaoyou and Nanjing stations, the threshold is very high, indicating the occurrence of severe extreme daily precipitation events in these regions (Fig. 2).

For the scale parameter, we found a similar spatial pattern as that for the threshold of daily precipitation extremes (Fig. 3). In addition, the shape parameter of the GDP determines the upper tail of the distribution and consequently describes the behavior of the most unusual extreme events (Cid et al., 2016). The shape parameter is 0.09 ± 0.07 for the region as a whole. Locally, 14 of the 16 stations in the study area had a shape parameter greater than zero, indicating that the extreme daily precipitation events exhibit a heavy tail distribution at most of the

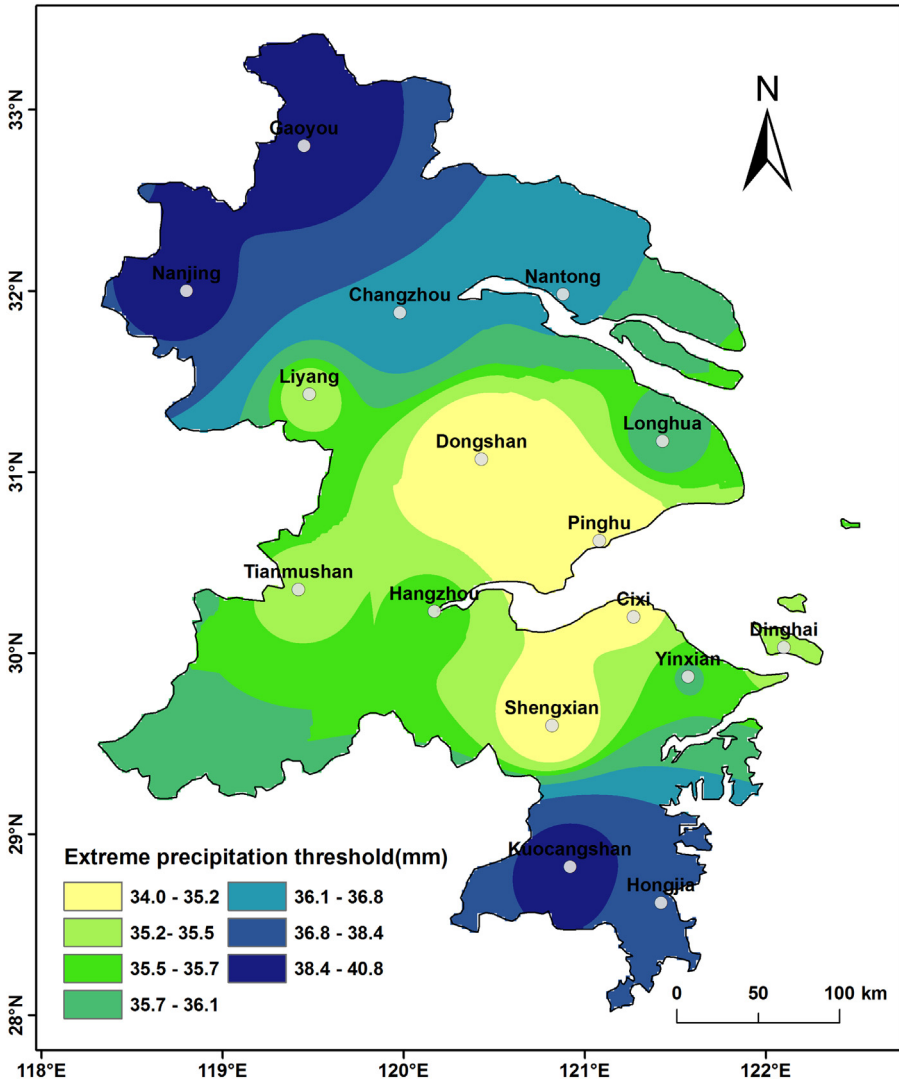


Fig. 2. Threshold precipitation amount of the POT approach in the YRD.

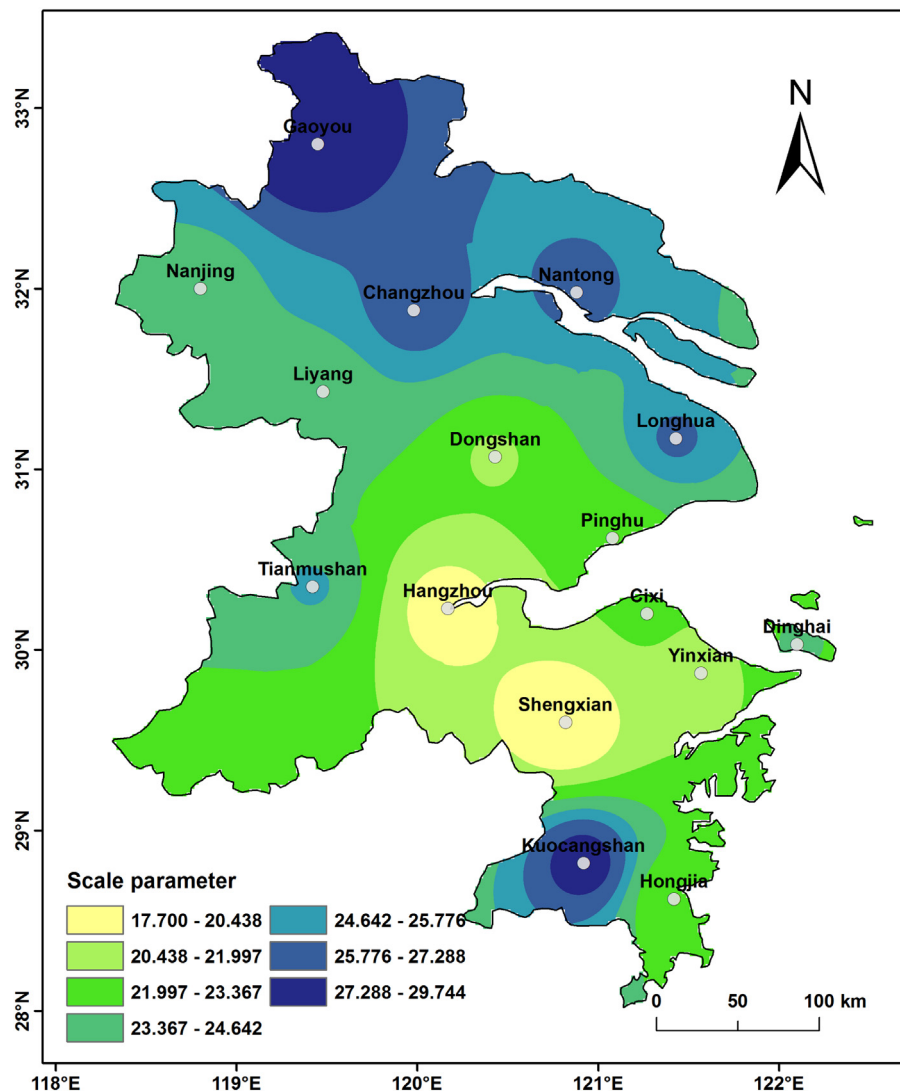


Fig. 3. Scale parameter of GPD in the YRD.

stations. Despite this result, negative values were found at Gaoyou station in Jiangsu Province, indicating a bounded upper tail at this station. This could be a consequence of either regularly-occurring intense extreme events or the scarce occurrence of extreme values. This is in accordance with the pattern of the threshold of the extreme daily precipitation events (Fig. 2). In addition, there is also a station with a shape parameter close to or equal to zero (i.e., that of Tianmushan station). This result indicates the exponential behavior of the upper tail and, therefore, higher magnitudes for the most unusual extreme events (Cid et al., 2016).

4.3. Gradual and abrupt trends in extreme daily precipitation events

Both gradual and abrupt trends in extreme daily precipitation events were analyzed in terms of both frequency and intensity. Taking the YRD as a whole, both the average values of *SDPI* and *SEPF* in the YRD showed an increasing trend from 1961 to 2012, at a rate of 0.041 mm/day ($P = 0.153$) and 0.017 days/year ($P = 0.003$), respectively (Fig. 7). The abrupt changes in extreme daily precipitation events were also examined for past decades. As shown in Fig. 7, the *SEPF* showed a mutation in the YRD at approximately 1981. In contrast, the change point of the *SDPI* occurred at approximately 1988 during past decades. Furthermore, the trends before- and after the change points were found to contrast with those of both the *SDPI* and *SEPF*. In detail,

the *SDPI* showed a significant decreasing trend prior to 1988 (-0.26 mm/day, $P = 0.000$), but an increasing trend after the change point (-0.14 mm/day, $P = 0.000$). Regarding the *SEPF*, it showed an increasing trend (0.003 days/year, $P = 0.910$) before 1981, but a negative trend (-0.012 days per year, $P = 0.150$) after the change point.

We further analyzed the spatial heterogeneities of the trends in extreme daily precipitation events under the condition of mononic change from 1961 to 2012, and we examined the abrupt changes during the periods before- and after the change points. As shown in Fig. 8a, the *SDPI* in most of the regions of the YRD showed an increase when assuming a monotonic trend from 1961 to 2012, at a rate of up to 2.663 mm/decade at Hongjia station. In addition, relatively large increasing trends could be found in Tianmushan, Changzhou, Pinghu, Nantong, Nanjing and Gaoyou, which were significant at the 0.05 level (Fig. 8a). However, the trends in the *SDPI* over the periods before- and after the change-point were different than the overall trends observed during the period of 1961–2012. In detail, the *SDPI* showed decreasing trends at most of the stations prior to the change point (Fig. 8b). However, increasing trends could be found in large parts of the YRD during the period after the change point of the extreme precipitation events (Fig. 8c).

For the extreme precipitation frequency, the *SEPF* in most of the regions of the YRD showed significant increasing trends except for those at Gaoyou, Liyang and Changzhou stations, when assuming a

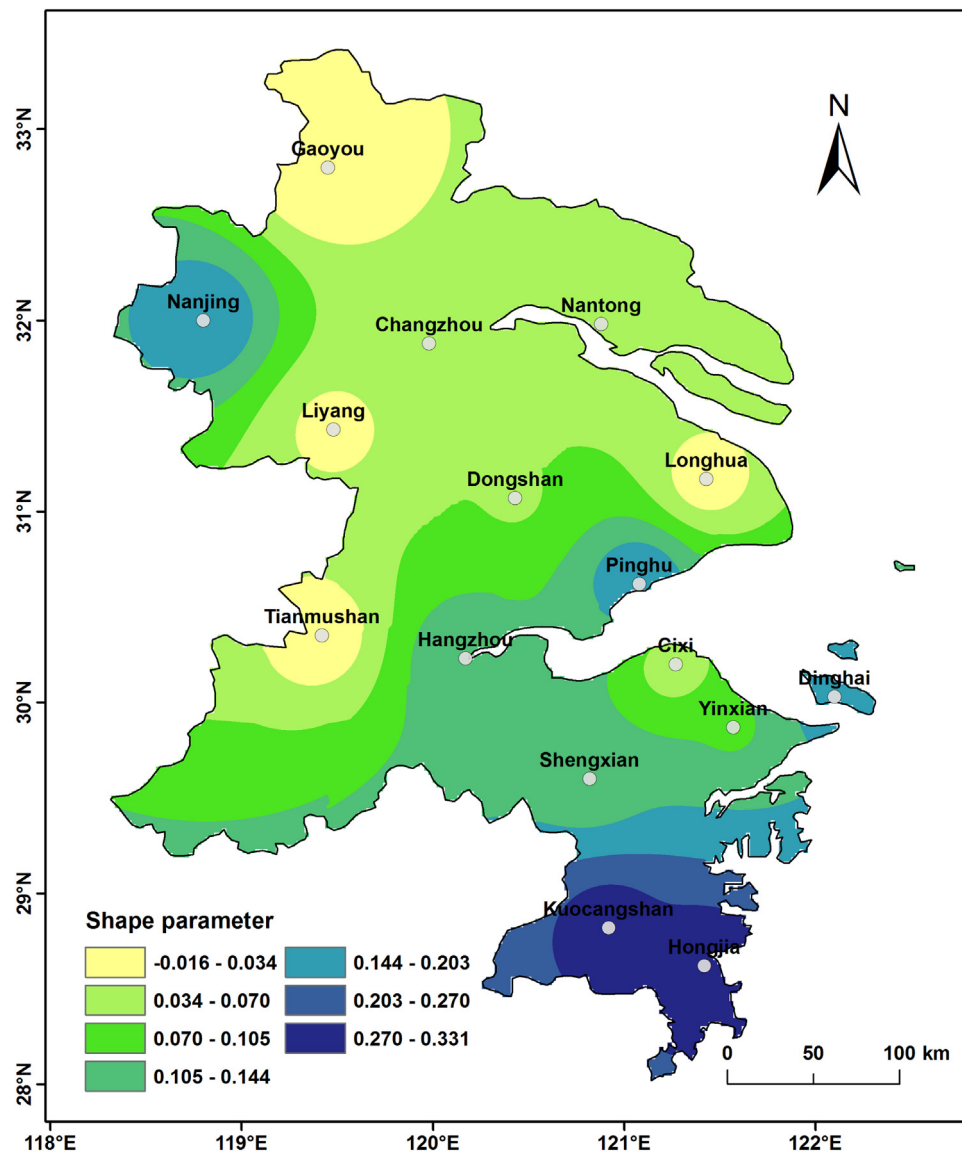


Fig. 4. Shape parameter of GPD in the YRD.

monotonic trend during the period of 1961–2012 (Fig. 9a). Regarding the abrupt changes, a similar pattern in trends could be found in the YRD before the change point (Fig. 9b). However, the trends at many stations were reversed after the change point under the condition of abrupt changes (Fig. 9c).

4.4. Daily precipitation extremes for different return periods

Figs. 5–6 show daily precipitation extremes for different return periods (i.e., 30 years and 50 years). The spatial distribution of the precipitation amount for the different return periods is consistent with the shape parameter of the fitted GPD model of extreme daily precipitation events (Fig. 4). Similar spatial patterns of daily precipitation extremes can be found for different return periods, but the changes are even greater. For instance, the differences in the daily precipitation extremes between the 30-year return periods and 50-year return periods reached maximum values as high as 200 mm in the southern parts of the Yangtze River Delta, where the shape parameters are also the largest in the whole YRD (Fig. 4). However, this difference is only 33 mm in the central parts of the regions with small shape parameters. Thus, regional analyses of precipitation extreme events for different return periods are needed to conduct planning and minimize the risk of

losses in the future.

5. Discussions

5.1. Trend comparison between gradual and abrupt changes in extreme daily precipitation events

We further conducted a comparison of the trends from the aspects of monotonic change over the period of 1961–2012 and abrupt change for the periods before- and after the change points. Regarding extreme precipitation intensity, the regional total *SDPI* showed a significant decreasing trend prior to the corresponding change point, and an increase after this time period. However, a Mann–Kendall analysis under a monotonic trend assumption suggested an increasing trend, although it was not significant. This difference could be associated with the even higher precipitation extremes from 1961 to 1963 (Fig. 7), which led to a distorted view of the trend detection. This phenomenon was also obvious from the spatial distribution of the *SDPI* changes. That is, the slope of the *SDPI* in the YRD for the whole period could be even smaller than that during the period after the change point. (Fig. 8a and c).

Regarding extreme precipitation frequency, the trends in the regional total *SEPF* showed a conflict when assuming a monotonic trend

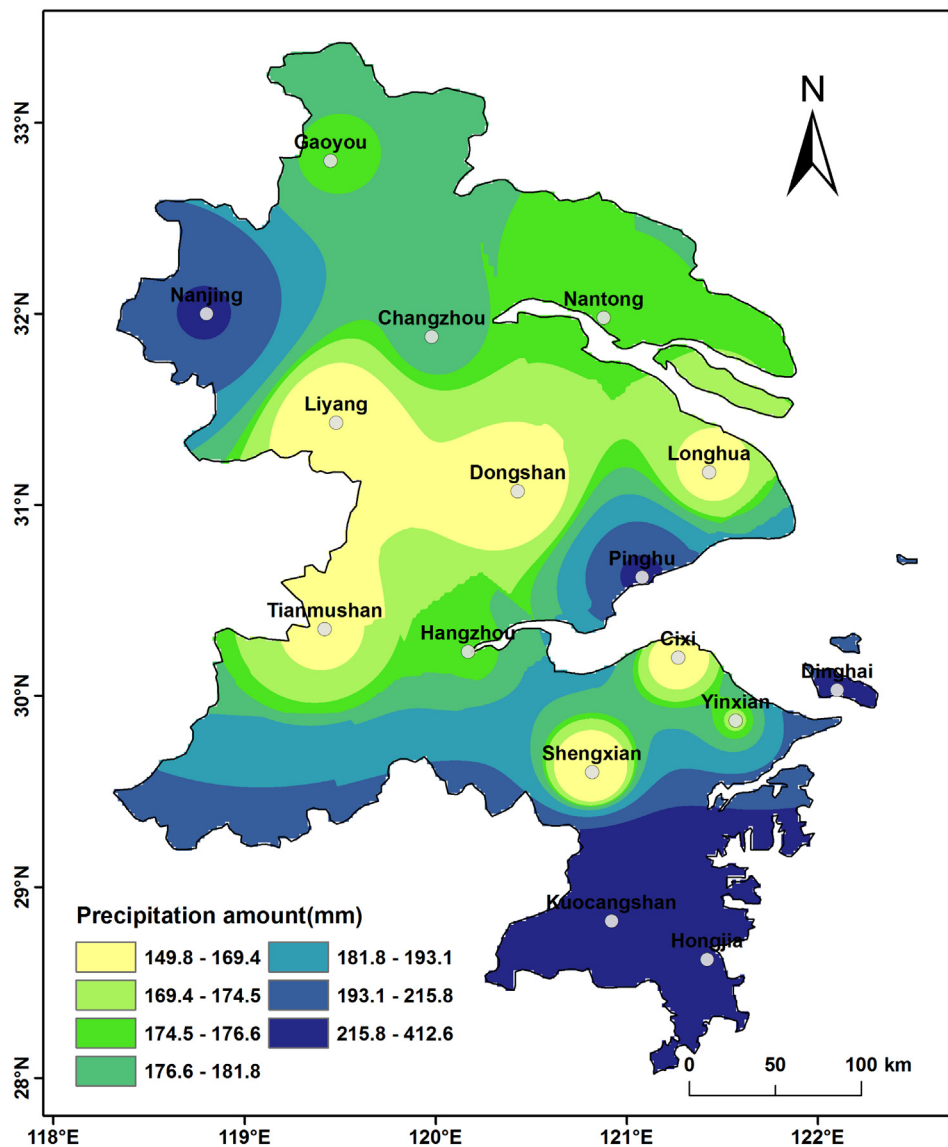


Fig. 5. Daily precipitation extremes for a 30-year return period during 1961–2012.

over the whole period or abrupt changes over the period before- and after the change point. In detail, the abrupt change in the average *SEPF* over the period of 1961–2012 might have caused a significant increasing trend when assuming a monotonic trend for the whole period (Fig. 7). The decreasing trends of the *SEPF* at some stations, including Nanjing, Dongshan, Pinghu and Hangzhou after the change points, could be overwhelmed by the increased trends over the whole time period in the YRD.

5.2. Relationships between changes in extreme daily precipitation events and the east Asian summer monsoon (EASM)

As indicated in Fig. 10, a relatively stronger EASM was found prior to 1975. A downward trend in the EASMI was found, at a rate of -0.165 per decade over the period 1961–2012 (Fig. 10). The EASM might exert great impacts on extreme daily precipitation events in the YRD over the period of 1961–2012. For example, a positive correlation could be found between the EASMI and *SDPI* ($R = 0.271$; $N = 52$; $P = 0.052$) when assuming a monotonic change in extreme precipitation events. This correlation was also confirmed in the analysis of the abrupt change of extreme daily precipitation events. In detail, a positive correlation could be found between the EASMI and the *SDPI* prior to

1988, a period with a stronger monsoon ($R = 0.752$; $N = 28$; $P = 0.000$). This correlation might be associated with the water sources of summer rainfall in the YRD provided by the EASM from the Pacific Ocean. In contrast, a negative correlation could be found after 1988 ($R = -0.172$; $N = 25$; $P = 0.420$), as the EASM weakened during this period (Fig. 10). This phenomenon could be explained by the frequent occurrence of rainfall under the condition of a weaker summer monsoon in the YRD (Li and Zeng, 2002; Ding et al., 2008). That is, the weaker EASM limited the northward extension of the summer monsoon to northern China, causing frequent occurrences of extreme daily precipitation events (Ding et al., 2008; Zhang et al., 2009; Zhang, 2015).

In contrast, a negative correlation between the EASMI and *SEPF* was found by assuming a monotonic trend over the period of 1961–2012 ($R = -0.152$; $N = 52$; $P = 0.282$). This result was in accordance with the findings of negative-correlations between the EASMI and summer rainfall in the middle and lower reaches of the Yangtze River in China. This phenomenon could be associated with the change in the EASM during the past decades. This result was in accordance with changes in the correlation after the change point of the extreme precipitation events over the period 1981–2012 ($R = -0.407$; $N = 32$; $P = 0.021$). In addition, a positive correlation between the EASMI and *SEPF* was significant during the period before the change point ($R = 0.595$;

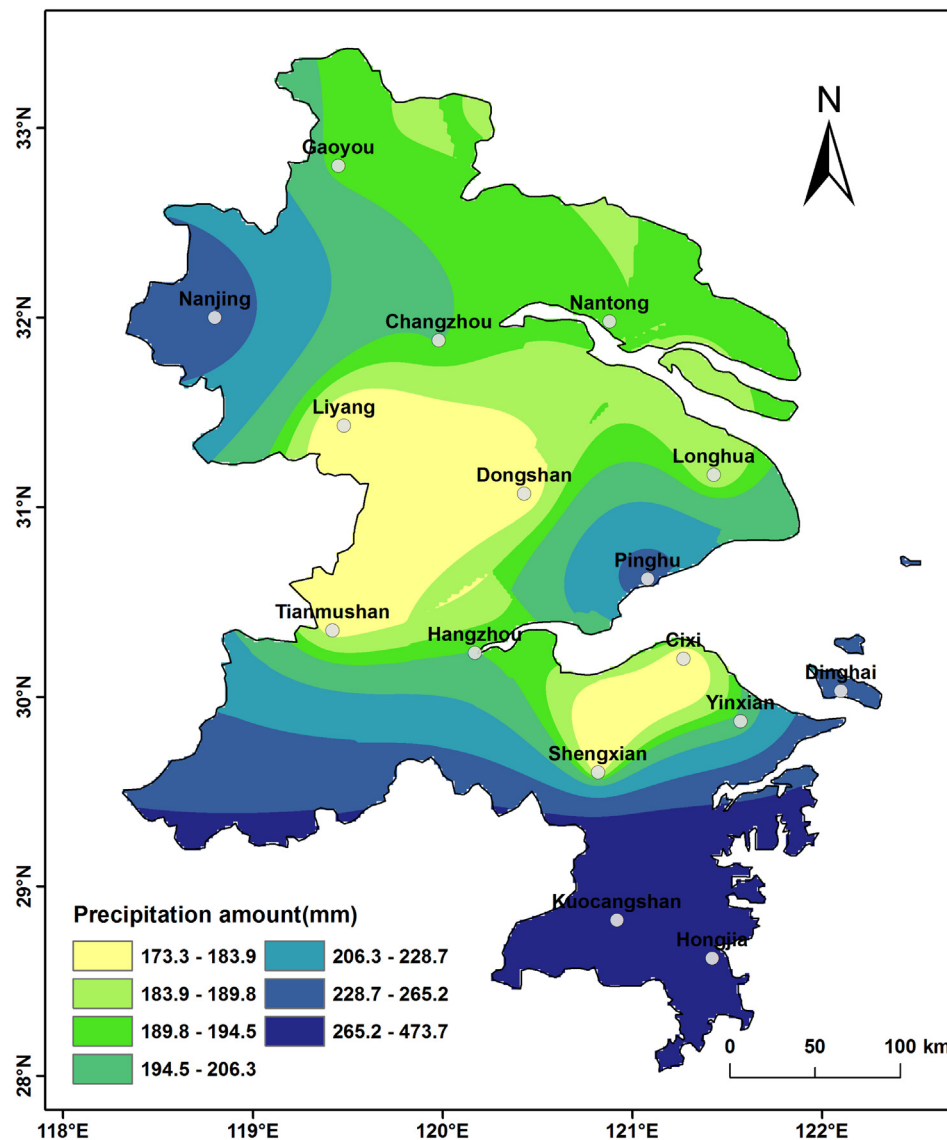


Fig. 6. The same as Fig. 5, but for a 50-year return period.

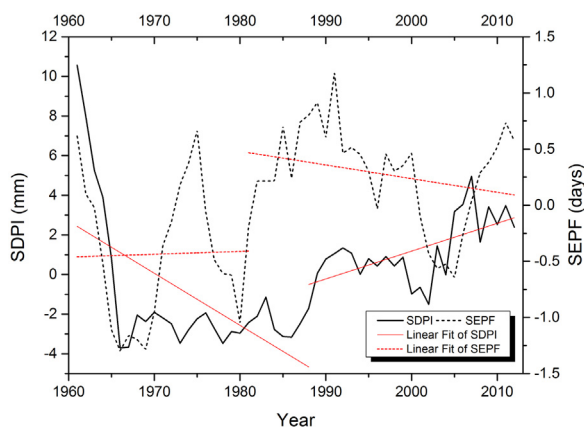


Fig. 7. Changes in SDPI and SEPF from 1961 to 2012.

$N = 21$; $P = 0.004$). This positive correlation might be associated with a stronger monsoon during this period (i.e., from 1961 to 1965) (Fig. 10).

5.3. Typhoon effects on changes in extreme daily precipitation events

Typhoons frequently result in enormous rainfall amounts in coastal regions, including the Yangtze River Delta in China. We found that there were no typhoons in the YRD prior to 1977. In addition, the number of times the stations were covered by a typhoon area of 30 kt winds increased from the southeastern to the northwestern YRD. The occurrence rate of extreme precipitation events varied from 87% at Hongjia station to 15% at Nanjing station from 1961 to 2012. To elucidate the effects of typhoons on extreme daily precipitation events, statistical analyses were conducted using time series of typhoon data from the aspects of temporal- and spatial changes. Spatially, a significant correlation was found between the number of typhoons and the SEPF using the average observed records from 16 stations in the YRD ($R = 0.668$; $N = 16$; $P = 0.005$). A weak correlation could be found between the number of typhoons and the SDPI ($R = 0.201$; $N = 16$; $P = 0.456$). We further examined the relationships between temporal changes in extreme daily precipitation events and the number of typhoons during the period of 1961–2012. Considering the frequent occurrence of typhoons, Hongjia station was selected as a typical sample to detect the effects of typhoons on extreme daily precipitation events. The records with typhoon occurrences, particularly during the period

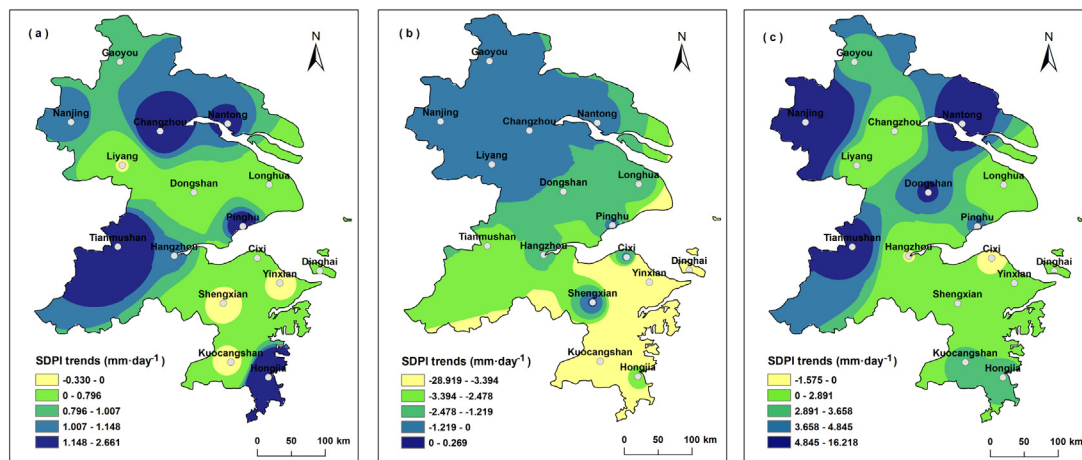


Fig. 8. Spatial distribution of the SDPI trends and the significance level in the YRD from 1961 to 2012: (a) for the whole time period, (b) before the change points and, (c) after the change points. All trends were enlarged by 10 times normal values.

after the change point of extreme daily precipitation events, were employed in the analysis. Consequently, a weak correlation was found between the number of typhoons and extreme precipitation event frequency at Hongjia station ($R = 0.190$; $N = 20$; $P = 0.422$). A similar correlation was found between the number of typhoons and extreme precipitation intensity at this station ($R = 0.361$; $N = 14$; $P = 0.205$). These weak correlations could be associated with the low occurrence of typhoons in comparison to extreme precipitation events. The results indicate the probable effects of typhoons on extreme precipitation events in the YRD.

5.4. Impacts of urban land use on changes in extreme daily precipitation

To represent the urbanization level, nighttime light images were employed to represent urban land use in the YRD. To mitigate the effects of other factors (e.g., typhoons and topography) on extreme daily precipitation events, eight stations on flat terrain in the northern parts of the YRD were used to explore the relationship between extreme daily precipitation events and urban land use.

Using nighttime light data from DMSP/OLS as a surrogate of urban land use, we found a positive correlation between the mean value of the DMSP/OLS images in urban areas and the SDPI ($R = 0.216$; $N = 8$; $P = 0.607$). For extreme precipitation event frequency, a negative correlation could also be found between the DMSP/OLS records and the SEPF ($R = -0.365$; $N = 8$; $P = 0.374$). Despite not being significant, these correlations indicate that large-scale urban land uses might increase the intensity of extreme daily precipitation events (e.g., around Longhua station in Shanghai, Fig. 8), but decrease the extreme precipitation event frequency (e.g., at Changzhou, Liyang and Gaoyou stations, Fig. 9). The increased intensity could be associated with the effects of an urban heat island and barrier effects of city buildings over large-scale urban lands in the YRD (Jiang and Liu, 2007; Wan and Zhong, 2014; Zhou et al., 2015). First, because of the low pressure produced by the warm air in the urban center, the colder air converged to the warmer area from the rural area. When the warm air meets the cold air from rural areas, precipitation could be increased down-wind of the urban area (Jiang and Liu, 2007). In addition, precipitation movement in the urban area could be slowed down because of the blocking effect of tall buildings on a large-scale in urban clusters, which act as a single large city. Consequently, precipitation might start later but is stronger than normal because of these urban effects (Bornstein and Lin, 2000; Wan and Zhong, 2014). However, because of the low evaporation in urban areas from the replacement of natural vegetation by impervious surface, the occurrence of extreme daily precipitation events might become less frequent in large-scale urban areas (Zhou et al.,

2015).

6. Conclusions

In this study, extreme daily precipitation events from 1961 to 2012 in the YRD were analyzed by fitting the threshold exceedances of daily precipitation as a generalized Pareto distribution. Gradual and abrupt changes in the extreme daily precipitation events were detected and attributed to aspects of the Eastern Asian Summer Monsoon, typhoons and large-scale urban land use. The results showed conflicting trends in the YRD when assuming a monotonic change over the whole period, as well as abrupt changes over the periods before and after the change point of the extreme daily precipitation events. This finding highlights the importance of the simultaneous analysis of gradual and abrupt changes when detecting the trends of extreme daily precipitation events. In addition, the analysis of extreme daily precipitation events during different return periods suggests the need to perform the regional analysis of daily precipitation extremes for multiple return periods to minimize the risk of loss from the extreme daily precipitation event under global climate change. The trend attribution of extreme precipitation changes in the YRD suggests the importance of the effects of EASM, as well as local factors (e.g., typhoons and urbanization) on extreme precipitation changes.

In addition, past studies have shown that extreme precipitation events over the Yangtze River Basin were associated with global air–sea heat fluxes and moisture transport (Gao and Xie, 2014; Gao et al., 2016). This study preliminarily analyzed the relationships between extreme daily precipitation events and the East Asian summer monsoon, typhoons, and urban land uses in the YRD. In future studies, we will explicitly examine the causes of the changes in the extreme daily precipitation events in the YRD by using regional climatic models from the aspects of large-scale circulation, urban expansion, local topography, etc.

Acknowledgement

We are heartily grateful to Dr. Juraj Parajka, his comments significantly improved this article. This study was supported by National Natural Science Foundation of China (Grant No. 41401438), National Students' Project for Innovation Training Program of China (Grant No. 201710320030) and a Project Funded by the Priority Academic Program Development of Jiangsu Higher Education Institutions.

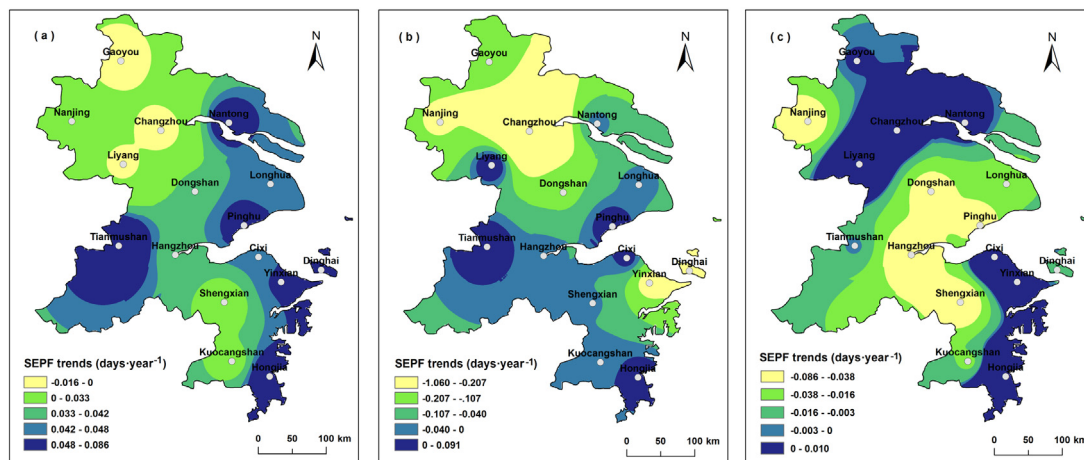


Fig. 9. The same as Fig. 8, but for the SEPF.

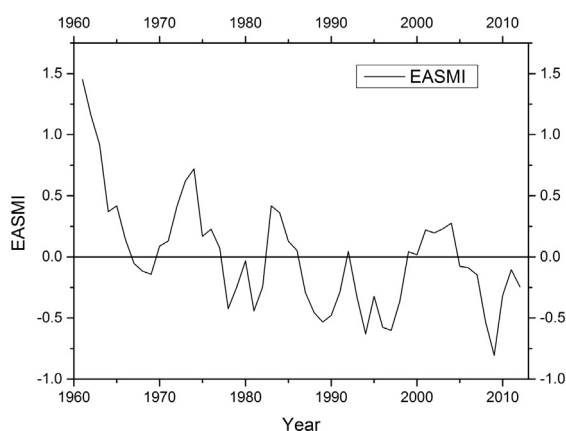


Fig. 10. Changes in the EASMI from 1961 to 2012.

References

- Acero, F.J., García, J.A., Gallego, M.C., 2011. Peaks-over-threshold study of trends in extreme rainfall over the Iberian peninsula. *J. Clim.* 24 (4), 1089–1105.
- Bornstein, R., Lin, Q., 2000. Urban heat islands and summertime convective thunderstorms in Atlanta: three case studies. *Atmos. Environ.* 34, 507–516.
- Cai, W., Borlace, S., Lengaigne, M., van Rensch, P., Collins, M., Vecchi, G., Timmermann, A., Santoso, A., McPhaden, M.J., Wu, L., 2014. Increasing frequency of extreme El Niño events due to greenhouse warming. *Nat. Clim. Chang.* (2), 111–116.
- Chang, C.P., Lei, Y., Sui, C.H., Lin, X., Ren, F., 2012. Tropical cyclone and extreme rainfall trends in East Asian summer monsoon since mid-20th century. *Geophys. Res. Lett.* 39, 18702.
- China Meteorological Administration (CMA), 1979. *Surface Meteorological Observation Standards*. China Meteorological Press, Beijing, China, pp. 167–192 (In Chinese).
- Cid, A., Menéndez, M., Castanedo, S., Abascal, A.J., Méndez, F.J., Medina, R., 2016. Long-term changes in the frequency, intensity and duration of extreme storm surge events in southern Europe. *Clim. Dyn.* 46, 1503–1516.
- Coles, S., Bawa, J., Trenner, L., Dorazio, P., 2001. *An Introduction to Statistical Modeling of Extreme Values*. Springer, London.
- Cunnane, C., 1973. A particular comparison of annual maxima and partial duration series methods of flood frequency prediction. *J. Hydrol.* 18, 257–271.
- Deidda, R., Puliga, M., 2009. Performances of some parameter estimators of the generalized Pareto distribution over rounded-off samples. *Phys. Chem. Earth Parts A/B/C* 34, 626–634.
- Ding, Y., Wang, Z., Sun, Y., 2008. Inter-decadal variation of the summer precipitation in East China and its association with decreasing Asian summer monsoon. Part I: observed evidences. *Int. J. Climatol.* 28, 1139–1161.
- Donegan, S.P., Tucker, J.C., Rollett, A.D., Barmak, K., Groeber, M., 2013. Extreme value analysis of tail departure from log-normality in experimental and simulated grain size distributions. *Acta Mater.* 61, 5595.
- Ehsanzadeh, E., Ouarda, T.B.M.J., Saley, H.M., 2015. A simultaneous analysis of gradual and abrupt changes in Canadian low streamflows. *Hydrol. Process.* 25 (5), 727–739.
- Elquliti, S., Alfalah, S.M., Alghamdi, M., Alabdali, Y., Ahmed, Alrowaily, 2016. Assessment of the frequency and return period for extreme rainfall causing floods in Mecca, Saudi Arabia. *Int. J. Sci. Tech. Res. Eng.* 1, 1–5.
- Gao, T., Xie, L., 2014. Multivariate regression analysis and statistical modeling for summer extreme precipitation over the Yangtze River basin, China. *Adv. Meteorol.* 2014.
- Gao, T., Xie, L., Liu, B., 2016. Association of extreme precipitation over the Yangtze River basin with global air–sea heat fluxes and moisture transport. *Int. J. Climatol.* 36, 3020–3038.
- GCESS (Global Change and Earth System Science), 2017. Available at: <http://ljp.gcess.cn/dct/page/65544>, Accessed date: 9 August 2017.
- Greenwood, J.A., Landwehr, J.M., Matalas, N.C., Wallis, J.R., 1979. Probability weighted moments: definition and relation to parameters of several distributions expressible in inverse form. *Water Resour. Res.* 15 (5), 1049–1054.
- Han, L., Xu, Y., Pan, G., Deng, X., Hu, C., Xu, H., Shi, H., 2015. Changing properties of precipitation extremes in the urban areas, Yangtze River Delta, China, during 1957–2013. *Nat. Hazards* 79, 437–454.
- Heisler White, J.L., Blair, J.M., Kelly, E.F., Harmoney, K., Knapp, A.K., 2009. Contingent productivity responses to more extreme rainfall regimes across a grassland biome. *Glob. Chang. Biol.* 15 (12), 2894–2904.
- Herold, N., Behrangi, A., Alexander, L.V., 2016. Large uncertainties in observed daily precipitation extremes over land. *J. Geophys. Res. Atmos.* 122, 668–681.
- Hipel, K.W., McLeod, A.I., 2005. *Time Series Modelling of Water Resources and Environmental Systems*. Electronic reprint of our book originally published in 1994. <http://www.stats.uwo.ca/faculty/aim/1994Book/>.
- Hirsch, R.M., Slack, J.R., Smith, R.A., 1982. Techniques of trend analysis for monthly water quality data. *Water Resour. Res.* 18, 107–121.
- Hosking, J.R., 1990. L-moments analysis and estimation of distributions using linear combinations of order statistics. *J. R. Stat. Soc. Ser. B Methodol.* 105–124.
- Houghton, J.T., et al., 2001. *Climate change 2001: the scientific basis*. In: Contribution of Working Group I to the Third Assessment Report of the International Panel on Climate Change. Cambridge University Press, United Kingdom and New York, NY, USA.
- Hu, C., Xu, Y., Han, L., Yang, L., Xu, G., 2016. Long-term trends in daily precipitation over the Yangtze River Delta region during 1960–2012, eastern China. *Theor. Appl. Climatol.* 125, 131–147.
- IPCC, 2012. *Managing the Risks of Extreme Events and Disasters to Advance Climate Change Adaptation: Special Report of the Intergovernmental Panel on Climate Change*. Cambridge University Press, Cambridge, UK and New York, NY, USA.
- Jiang, X., Liu, W., 2007. Numerical simulations of impacts of urbanization on heavy rainfall in Beijing using different land-use data. *J. Met. Res.* 21, 245–255.
- Kim, N.H., Ramu, P., Queipo, N.V., 2006. Tail modeling in reliability-based design optimization for highly safe structural systems. *AIAA* 1–11.
- Lang, M., Ouarda, T., Bobée, B., 1999. Towards operational guidelines for over-threshold modeling. *J. Hydrol.* 225, 103–117.
- Li, J., Zeng, Q., 2002. A unified monsoon index. *Geophys. Res. Lett.* 29, 111–115.
- Li, J.P., Wu, Z.W., Jiang, Z.H., He, J.H., 2010. Can global warming strengthen the East Asian summer monsoon? *J. Clim.* 23, 6696–6705.
- Lupikasza, E., 2016. *Definitions and Indices of Precipitation Extremes*. Springer International Publishing.
- NCEI (National Centers for Environmental Information), 2017. Available at: <https://ngdc.noaa.gov/eog/download.html>, Accessed date: 9 August 2017.
- Neykov, N.M., Neytchev, P.N., Zucchini, W., 2014. Stochastic daily precipitation model with a heavy-tailed component. *Nat. Hazards Earth Syst. Sci.* 2, 2321–2335.
- Palutikof, J.P., Brabson, B.B., Lister, D.H., Adcock, S.T., 1999. A review of methods to calculate extreme wind speeds. *Meteorol. Appl.* 6 (2), 119–132.
- Pei, F., Wu, C., Qu, A., Xia, Y., Wang, K., Zhou, Y., 2017. Changes in extreme precipitation: a case study in the middle and lower reaches of the Yangtze River in China. *Water* 9, 943.
- Pei, F., Wu, C., Liu, X., Li, X., Yang, K., Zhou, Y., Wang, K., Xu, L., Xia, G., 2018. Monitoring the vegetation activity in China using vegetation health indices. *Agric. For. Meteorol.* 248, 215–227.
- Pickands III, J., 1975. Statistical inference using extreme order statistics. *Ann. Stat.* 119–131.
- Pettitt, A.N., 1979. A Non-Parametric Approach to the Change-Point Problem. *J. R. Stat. Soc.* 28, 126–135.

- Pohlert, T., 2016. trend: Non-parametric Trend Tests and Change-point Detection, R Package Version 0.1.0. <https://CRAN.R-project.org/package=trend>.
- R Core Team, 2016. R: A Language and Environment for Statistical Computing. R Foundation for Statistical Computing, Vienna, Austria. <https://www.R-project.org/>.
- Ribatet, M., Dutang, C., 2016. A User's Guide to the POT Package (Version 1.0). <http://cran.r-project.org/>.
- RSMC (Regional Specialized Meteorological Center) Tokyo-Typhoon Center, 2017. Available at: <http://www.jma.go.jp/jma/jma-eng/jma-center/rsmc-hp-pub-eg/trackarchives.html>, Accessed date: 9 August 2017.
- Sarhadi, A., Souliis, E.D., 2017. Time-varying extreme rainfall intensity-duration-frequency curves in a changing climate. *Geophys. Res. Lett.* 5, 2454–2463.
- Schumacher, R.S., Davis, C.A., 2010. Ensemble-based forecast uncertainty analysis of diverse heavy rainfall events. *Weather Forecast.* 25, 1103–1122.
- Sen, P.K., 1968. Estimates of the regression coefficient based on Kendall's tau. *J. Am. Stat. Assoc.* 63, 1379–1389.
- Solomon, S., et al., 2007. Climate change 2007: the physical science basis. In: Contribution of Working Group I to the Fourth Assessment Report. Vol. 996 Cambridge University Press, Cambridge, United Kingdom and New York, NY, USA.
- Su, B., Gemmer, M., Jiang, T., 2008. Spatial and temporal variation of extreme precipitation over the Yangtze River basin. *Quat. Int.* 186 (1), 22–31.
- Sunyer, M.A., Hundecha, Y., Lawrence, D., Madsen, H., Willems, P., Martinkova, M., Vermoor, K., Bürger, G., Hanel, M., Kriaučiūnienė, J., Loukas, A., Osuch, M., Yücel, I., 2015. Inter-comparison of statistical downscaling methods for projection of extreme precipitation in Europe. *Hydrol. Earth Syst. Sci.* 19, 1827–1847.
- Taylor, R.G., et al., 2013. Evidence of the dependence of groundwater resources on extreme rainfall in East Africa. *Nat. Clim. Chang.* 3 (4), 374–378.
- Tedeschi, R.G., Grimm, A.M., Cavalcanti, I.F.A., 2016. Influence of central and east ENSO on precipitation and its extreme events in South America during austral autumn and winter. *Int. J. Climatol.* 36, 4797–4814.
- Tomczyk, A.M., White, P.C.L., Ewertowski, M.W., 2015. Effects of extreme natural events on the provision of ecosystem services in a mountain environment: the importance of trail design in delivering system resilience and ecosystem service co-benefits. *J. Environ. Manag.* 166, 156.
- Typhoon Committee, 2008. Typhoon Committee Operational Manual: Meteorological Component. 5 World Meteorological Organization.
- Valadares Tavares, L., Evaristo Da Silva, J., 1983. Partial duration series method revisited. *J. Hydrol.* 64, 1)–1–14.
- Villarini, G., Smith, J.A., Vecchi, G.A., 2013. Changing frequency of heavy rainfall over the Central United States. *J. Clim.* 26.
- Wan, H., Zhong, Z., 2014. Ensemble simulations to investigate the impact of large-scale urbanization on precipitation in the lower reaches of Yangtze River valley, China. *Q. J. R. Meteorol. Soc.* 140, 258–266.
- Wang, Q.J., 1991. The POT model described by the generalized Pareto distribution with Poisson arrival rate. *J. Hydrol.* 129 (1), 263–280.
- Wang, B., Wu, Z., Li, J., Liu, J., Chang, C.P., Ding, Y., Wu, G., 2008. How to measure the strength of the East Asian summer monsoon. *J. Clim.* 21, 4449–4463.
- Wang, L., Wu, Z., He, H., Wang, F., Du, H., Zong, S., 2016. Changes in summer extreme precipitation in Northeast Asia and their relationships with the East Asian summer monsoon during 1961–2009. *Int. J. Climatol.* 37, 25–35.
- Wu, F.T., Wang, S.Y., Fu, C.B., Qian, Y., Gao, Y., Lee, D.K., Cha, D.H., Tang, J.P., Hong, S., 2016. Evaluation and projection of summer extreme precipitation over East Asia in the regional model inter-comparison project. *Clim. Res.* 69, 45–58.
- Yang, Y., Tian, F., 2009. Abrupt change of runoff and its major driving factors in Haihe River catchment, China. *J. Hydrol.* 374, 373–383.
- Yang, S.Y., Sun, F.H., Jian-Zhong, M.A., 2008. Evolution of precipitation extremes in Northeast China on the background of climate warming. *Sci. Geogr. Sin.* 28, 224–228 (In Chinese).
- Yin, Y., Chen, H., Xu, C.Y., Xu, W., Chen, C., Sun, S., 2016. Spatio-temporal characteristics of the extreme precipitation by L-moment-based index-flood method in the Yangtze River Delta region, China. *Theor. Appl. Climatol.* 124, 1005–1022.
- Zhai, P., Zhang, X., Wan, H., Pan, X., 2005. Trends in total precipitation and frequency of daily precipitation extremes over China. *J. Clim.* 18, 1096–1108.
- Zhang, R., 2015. Changes in east Asian summer monsoon and summer rainfall over eastern China during recent decades. *Sci. Bull.* 60, 1222–1224.
- Zhang, Z.X., Luan, Y.L., Jiang, T., Zhang, Q., Zeng, Y., 2008. Changes of extreme precipitation in the Yangtze River delta and its pre-evaluation for future. *J. Nanjing For. Univ.* 32, 5–8.
- Zhang, Q., Xu, C.Y., Becker, S., Zhang, Z.X., Chen, Y.D., Coulibaly, M., 2009. Trends and abrupt changes of precipitation maxima in the Pearl River basin, China. *Atmos. Sci. Lett.* 10, 132–144.
- Zhang, Q., Li, J., Singh, V.P., Xu, C.Y., 2013. Copula-based spatio-temporal patterns of precipitation extremes in China. *Int. J. Climatol.* 33, 1140–1152.
- Zhou, L., Jiang, Z., Zhaoxin, L.L., Yang, X., 2015. Numerical simulation of urbanization climate effects in regions of East China. *Chin. J. Atmos. Sci.* 39, 596–610.